

We are IntechOpen, the world's leading publisher of Open Access books Built by scientists, for scientists

5,500

Open access books available

136,000

International authors and editors

170M

Downloads

Our authors are among the

154

Countries delivered to

TOP 1%

most cited scientists

12.2%

Contributors from top 500 universities



WEB OF SCIENCE™

Selection of our books indexed in the Book Citation Index
in Web of Science™ Core Collection (BKCI)

Interested in publishing with us?
Contact book.department@intechopen.com

Numbers displayed above are based on latest data collected.
For more information visit www.intechopen.com



Shock Tube Combustion Analysis

Claudio Marcio Santana and Jose Eduardo Mautone Barros

Abstract

The shock tube is a metal tube that the gas at low pressure and high pressure are separated by a diaphragm. When the diaphragm (made of material copper and aluminum) breaks on predetermined conditions (high pressure in this case) produces shock waves that move from the high-pressure chamber (known the compression chamber or Driver section) for low pressure chamber (known the expansion chamber or Driven section). The objective of this work is to correlate the ignition delay times of conventional Diesel and Biodiesel from soybean oil measured in a shock tube. The results were correlated with the cetane number of respective fuels and compared with the ignition delay times of Diesel and Biodiesel with cetane numbers of known. The ignition delay time of biodiesel from soybean oil was approximately three times greater than the ignition delay time of conventional Diesel. The contribution of this work is that it shows why pure biodiesel should not be used as substitutes for Diesel compression ignition engines without any major changes in the engines.

Keywords: diesel ignition delay time, biodiesel ignition delay time, shock tube, diesel cetane number, biodiesel from soybean oil cetane number

1. Introduction

Shock tube is an equipment used to study gas flow in different areas of engineering and operating conditions, such as: shock wave movement, aerodynamic flows under different temperature and pressure conditions, gas compressibility and fuel combustion. The equipment is constructed by a metal tube separated by a diaphragm, which divides the equipment into two sections. The high-pressure section is called the driver section while the low-pressure section is called the driven section. The diaphragm separating the two sections is designed to withstand a certain pressure, when that pressure is reached the diaphragm breaks and a compression wave is formed and moves towards the driven section. Instantly an expansion wave is formed and propagates towards the driver section. This movement of the gas mass inside the shock tube causes an increase in pressure and temperature in the driven section and a reduction in pressure and temperature in the driver section, [1, 2]. The **Figure 1** shows the driver and driven sections of shock tube before the rupture of the diaphragm.

After the diaphragm rupture is formed inside the shock tube, the contact surface, a region that did not feel the passage of the shock wave, a second region that felt the effects of the passage of the shock wave, a third region that did not feel the passage of the expansion wave and a fourth region that felt the effects of the expansion wave passage, [2, 4]. The **Figure 2** shows the contact surfaces and four regions formed after the diaphragm rupture.

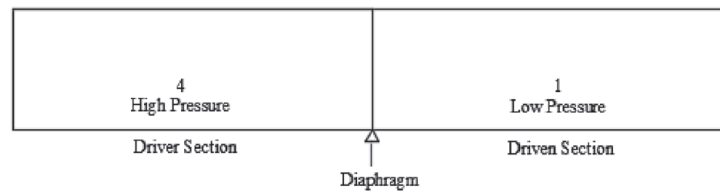


Figure 1. Driver and driven sections of the shock tube before rupture of the diaphragm (adapted from [3]).

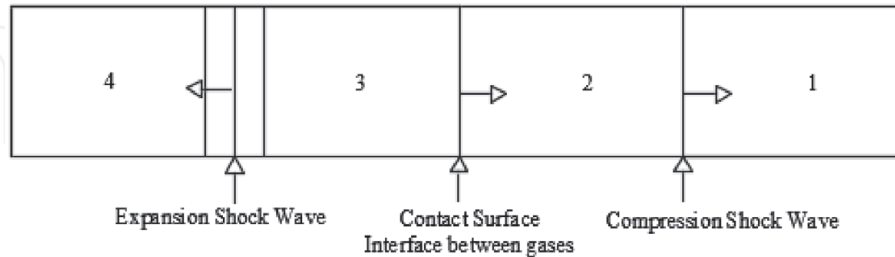


Figure 2. Contact surfaces and four regions formed after the diaphragm rupture (adapted from [3]).

The incident shock wave is reflected and propagates towards the driver section when it reaches the closed end of the shock tube driven section. The reflected shock wave superimposes the motion of the incident shock wave, this superposition increases temperature and pressure in the driven section. The reflected shock wave is responsible for causing the dissociation and ionization of the gas inside the shock tube, [2, 4]. The **Figure 3** shows the propagation shock wave, reflected wave, expansion wave, reflected expansion wave and the contact surface after the diaphragm rupture shock tube.

The shock force is determined by the pressure ratio (P_4/P_1) and speed of sound propagation (a_4/a_1) between the driver and driven sections, [3]. The **Figure 4** shows the conditions of pressure and temperature in the driver and driven sections before the diaphragm rupture.

In the front of the shock and expansion waves the pressure, density and temperature do not varied in relation to the initial conditions in the driver and driven

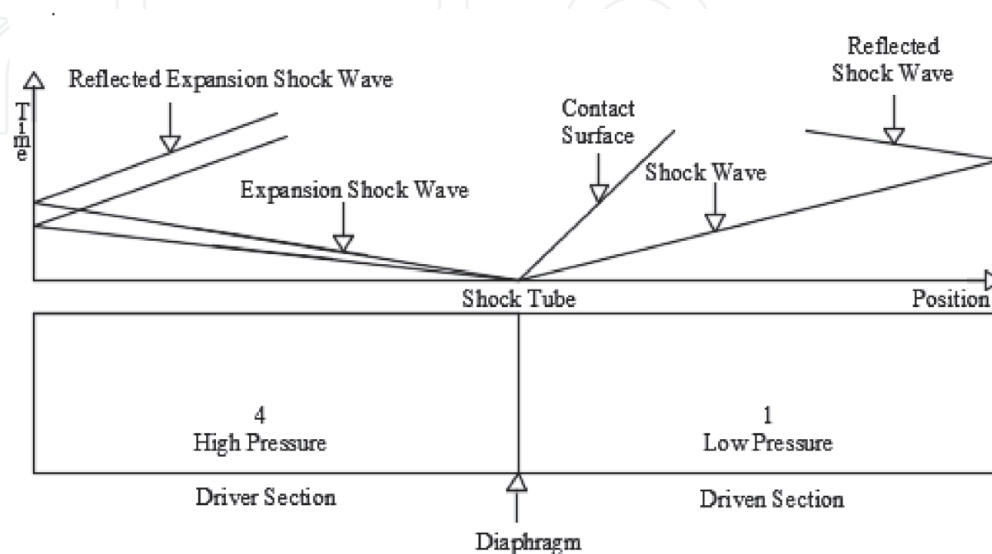


Figure 3. Shock wave, reflected wave, expansion wave, reflected expansion wave and the contact surface after the diaphragm rupture shock tube.

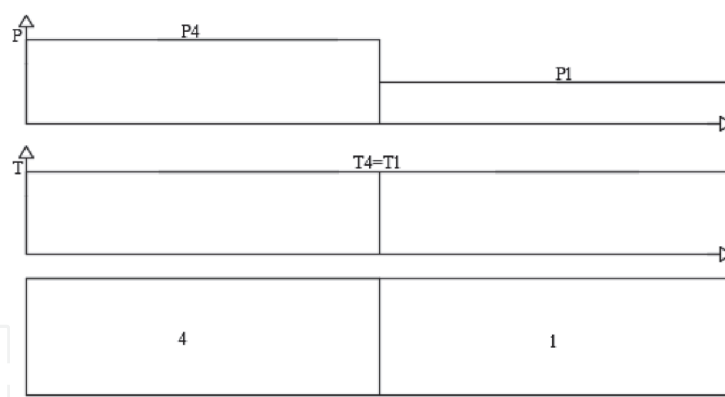


Figure 4. Condition of pressure and temperature in the driver and driven sections before the diaphragm rupture (adapted from [3]).

sections, these sections are not affected by the passage of the shock and expansion waves. Behind the shock wave, pressure, density and temperature increase, while behind the expansion wave these variables decrease, [3]. The **Figure 5** shows the conditions of pressure and temperature in the driver and driven sections after the diaphragm rupture.

The **Figure 6** shows the conditions of shock tube after reflection shock wave and reflection expansion wave.

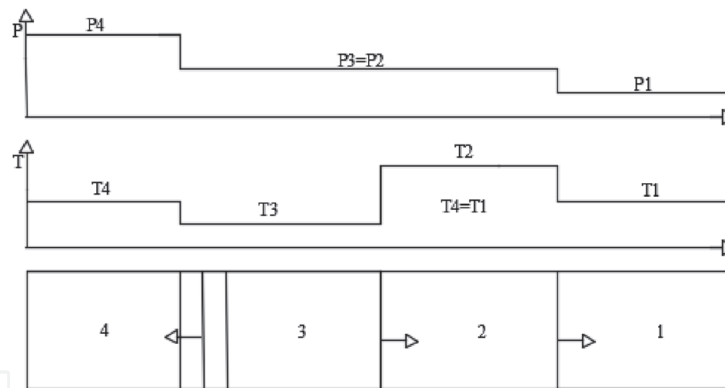


Figure 5. Condition of pressure and temperature in the driver and driven sections after the diaphragm rupture (adapted from [3]).

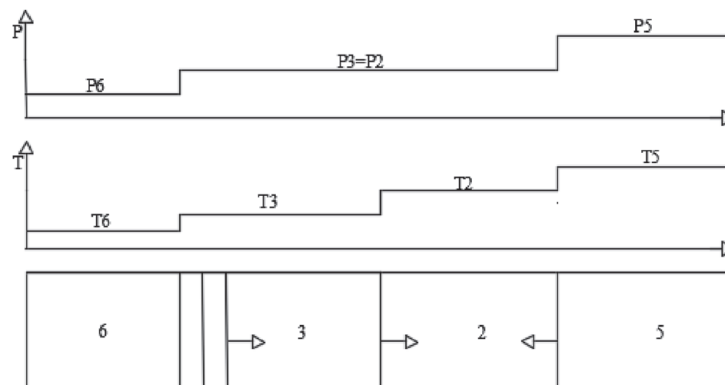


Figure 6. Conditions of shock tube after reflection shock wave and reflection expansion wave (adapted from [3]).

2. Analytical solution shock tube for ideal gas

The speed of sound for each state gas must be calculated using the Eq. (1).

$$a = \sqrt{\gamma RT} \quad (1)$$

Where γ is the ratio of specific heats of the gas, R is the universal gas constant and T is the gas temperature in the respective regions of the shock tube. The Mach number can be determined using the Eq. (2), [3].

$$\frac{P_4}{P_1} = \frac{\gamma_{1-1}}{\gamma_{1+1}} \left[\frac{2\gamma_1 M_s^2}{\gamma_{1-1}} - 1 \right] \left[1 - \frac{\frac{\gamma_{4-1}}{\gamma_{4+1}} \left(\frac{a_1}{a_4} \right) (M_s^2 - 1)}{M_s} \right]^{\frac{2\gamma_4}{\gamma_{4-1}}} \quad (2)$$

Where M_s is the shock wave Mach number, the subscript 1 denotes the properties of the driven section and the subscript 4 denotes the properties of the driver section. The pressure ratio (P_2/P_1) on both sides of the shock wave can be calculated using the Eq. (3), [3].

$$\frac{P_2}{P_1} = 1 + \frac{2\gamma_1}{\gamma_1 + 1} (M_s^2 - 1) \quad (3)$$

The pressure ratio (P_2/P_1) can be used to determine the temperature ratio (T_2/T_1) on both sides of the shock wave using the Eq. (4), [3].

$$\frac{T_2}{T_1} = \frac{P_2}{P_1} \left(\frac{\frac{\gamma_1 + 1}{\gamma_1 - 1} + \frac{P_2}{P_1}}{1 + \frac{\gamma_1 + 1}{\gamma_1 - 1} \frac{P_2}{P_1}} \right) \quad (4)$$

The shock wave reflected Mach number M_R depend the velocity of the incident shock wave and can be calculated by the Eq. (5), [3].

$$\frac{M_R}{M_R^2 - 1} = \frac{M_s}{M_s^2 - 1} \sqrt{1 + \frac{2(\gamma_1 - 1)}{(\gamma_1 + 1)^2} (M_s^2 - 1) \left(\gamma_1 + \frac{1}{M_s^2} \right)} \quad (5)$$

The increased pressure of the shock wave reflected P_5 depend the speed of the incident shock wave, this ratio can be calculated by the Eq. (6), [3].

$$\frac{P_5}{P_2} = 1 + \frac{2\gamma_1}{\gamma_1 + 1} (M_R^2 - 1) \quad (6)$$

The Eq. (7) shows the relationship of the motion of the mass gas behind the shock wave and the reflected shock wave, [3].

$$\frac{2a_1}{\gamma_1 + 1} \left(M_s - \frac{1}{M_s} \right) = \frac{2a_2}{\gamma_1 + 1} \left(M_R - \frac{1}{M_R} \right) \quad (7)$$

The calculations involving speed of the gas molecules can be determined by the Eq. (8), [3].

$$Mach\ M = \frac{V}{a} \quad (8)$$

The calculation of the speed of the shock wave can be determined by the Eq. (9), [3].

$$V_R = M_R a_2 - V_2 \quad (9)$$

To determine the relationship between reflected shock wave pressure and incident shock wave pressure using the Eq. (10), [3].

$$\frac{P_5}{P_2} = \left(\frac{\frac{\gamma_1+1}{\gamma_1-1} + 2 - \frac{P_1}{P_2}}{1 + \frac{\gamma_1+1}{\gamma_1-1} \frac{P_1}{P_2}} \right) \quad (10)$$

With the ratio compression known the ratio reflected shock wave temperature and incident shock wave temperature can be determined by Eq. (11), [3].

$$\frac{T_5}{T_2} = \frac{P_5}{P_2} \left(\frac{\frac{\gamma_1+1}{\gamma_1-1} + \frac{P_5}{P_2}}{1 + \frac{\gamma_1+1}{\gamma_1-1} \frac{P_5}{P_2}} \right) \quad (11)$$

The temperature and pressure behind the reflected shock wave can be calculated knowing only the Mach number of the incident shock wave. This value can be determined from the velocity of the gas driven and wave velocity, [3].

3. Works carried out in shock tube

[5] used a shock tube to measure the ignition delay times of mixture with ethanol, n-heptane and iso-octane and mixture with ethanol, iso-octane, n-heptane and toluene. The tests were performed at temperatures ranging from 690 to 1200 K and pressures at 10, 30 and 50 bar. For testing mixture with ethanol, n-heptane and iso-octane were found delay times ranging from 120 to 6230 microseconds, for testing mixture with iso-octane, toluene, n-heptane and ethanol were found delay times ranging from 28 to 8731 microseconds and for testing mixture with iso-octane, toluene and n-heptane were found ignition delay times ranging from 180 to 1060 microseconds. [6] also used a shock tube to measure the ignition delay times of mixture with n-heptane and n-butanol. The tests were performed at temperatures ranging from 1200 to 1500 K, pressures at 2 and 10 atm and equivalence ratios at 0.5 and 1. For testing with pure n-heptane were found delay times ranging from 90 to 1230 microseconds, for testing mixture with pure n-butanol were found delay times ranging from 120 to 950 microseconds and for testing mixture with n-heptane and n-butanol were found ignition delay times ranging from 30 to 1010 microseconds. [7] also conducted shock tube tests with n-heptane, iso-octane and ethanol. The tests were performed at temperatures ranging from 690 to 1200 K and pressures at 10, 30 and 50 bar. For testing at 10 bar and mixture with n-heptane, iso-octane and ethanol were found ignition delay times ranging from 181 to 2870 microseconds. For testing at 30 bar and mixture with n-heptane, iso-octane and ethanol were found ignition delay times ranging from 172 to 7800 microseconds. For testing at 50 bar and mixture with n-heptane, iso-octane and ethanol were found ignition delay times ranging from 115 to 7690 microseconds. For testing at 10 bar and mixture with n-heptane, iso-octane, toluene and di-isobutylene were found ignition delay times ranging from 245 to 4600 microseconds. For testing at 30 bar and mixture with n-heptane, iso-octane, toluene and di-isobutylene were found ignition delay times ranging from 191 to 8320 microseconds. For testing at 10 bar and mixture with n-heptane, iso-octane, toluene and di-isobutylene were

found ignition delay times ranging from 149 to 10100 microseconds. [8] also conducted shock tube tests with n-heptane and were found ignition delay times ranging from 1220 to 10600 microseconds. The tests were performed at temperatures ranging from 651 to 823 K, pressures at 6.1 and 7.4 atm and equivalence ratio of 0.75. [9] also conducted shock tube tests with propane and were found ignition delay times ranging from 100 to 11000 microseconds for testing at 6 atm. Were found ignition delay times ranging from 200 to 11000 microseconds for testing at 24 atm and were found ignition delay times ranging from 300 to 600 microseconds for testing at 60 atm. The tests were performed at temperatures ranging from 980 to 1400 K and equivalence ratio 0.5. [10] also conducted shock tube tests with methyl butanoate and were found ignition delay times ranging from 19630 to 24180 microseconds for testing at 10.2 atm. The tests were performed at temperatures from 985 K and equivalence ratio 0.3. [11] also conducted shock tube tests with methyl octanoate, n-nonane and methylcyclohexane. The tests were performed at temperatures ranging from 1263 to 1672 K, pressures at 1.5 and 10 atm and equivalence ratio 0.5, 1 and 2. For tests with equivalence ratio 0.5 at 1.5 atm were found for methyl octanoate ignition delay times ranging from 40 to 1000 microseconds, for n-nonane were found delay times ranging from 100 to 1100 microseconds and for methylcyclohexane were found delay times ranging from 100 to 1200 microseconds. For tests with equivalence ratio 0.5 at 10 atm were found for methyl octanoate ignition delay times ranging from 110 to 800 microseconds, for n-nonane were found delay times ranging from 90 to 900 microseconds and for methylcyclohexane were found delay times ranging from 90 to 1050 microseconds. For tests with equivalence ratio 1 at 1.5 atm were found for methyl octanoate ignition delay times ranging from 120 to 1000 microseconds, for n-nonane were found delay times ranging from 90 to 1100 microseconds and for methylcyclohexane were found delay times ranging from 120 to 1100 microseconds. For tests with equivalence ratio 1 at 10 atm were found for methyl octanoate ignition delay times ranging from 80 to 1000 microseconds, for n-nonane were found delay times ranging from 80 to 1100 microseconds and for methylcyclohexane were found delay times ranging from 150 to 1100 microseconds. For tests with equivalence ratio 2 at 1.5 atm were found for methyl octanoate ignition delay times ranging from 100 to 900 microseconds, for n-nonane and for methylcyclohexane were found delay times ranging from 100 to 1100 microseconds. For tests with equivalence ratio 2 at 10 atm were found for methyl octanoate and methylcyclohexane ignition delay times ranging from 90 to 1000 microseconds, for n-nonane were found delay times ranging from 100 to 1100 microseconds. [12] also conducted shock tube tests with methyl stearate, methyl oleate, methyl linoleate, methyl linolenate, and methyl palmitate and were found ignition delay times for all fuel testing ranging from 200 to 90000 microseconds for testing at 13.5 bar. The tests were performed at temperatures from 700 to 1100 K and equivalence ratio 1. [13] also conducted shock tube tests with jets fuels, rocket propellants, diesel fuel and gasoline fuel and were found ignition delay times for all fuel testing ranging from 100 to 1900 microseconds for testing at pressure from 6 to 60 atm. The tests were performed at temperatures from 1000 to 1400 K and equivalence ratio 0.85 and 1.15. [14] also conducted shock tube tests with mixture of biodiesel with diesel fuel and were found ignition delay times for all fuel testing ranging from 60 to 2600 microseconds for testing at pressure at 0.12 Mpa. The tests were performed at temperatures from 1174 to 1685 K and equivalence ratio 0.5, 1 and 1.5. [15] also conducted shock tube tests with diesel fuel and alternative hydro processed jet fuels. The tests were performed at temperatures from 650 to 1300 K, pressures from 0.8 to 80 atm and equivalence ratio 0.25 to 1.5. For testing with jet fuels were found ignition delay times ranging from 60 to 8000 microseconds and for testing with diesel fuels were found ignition delay times ranging from 90 to

4000 microseconds. [16] also conducted shock tube tests with conventional and alternative jet fuels, alcohol to jet, direct sugar to hydrocarbon, biodiesel-like fuel, n-heptane, n-dodecane, m-xylene and iso-dodecane. Were found ignition delay times for all fuel testing ranging from 20 to 3200 microseconds. The tests were performed at temperatures from 980 to 1800 K, pressures at 16 atm and equivalence ratio at 0.5.

4. Experimental measuring the ignition delay times of the convectional diesel and biodiesel from soybean oil using a shock tube

The experiments were conducted in the heated shock tube facility of the Mobility Technology Center (CTM) of Federal University of Minas Gerais (UFMG). The shock tube has a 3 m long driver section and a 3 m long driven section with an internal diameter of 97.20 mm. Aluminum diaphragm of 0.4 mm thickness divided the driver and driven sections before each experiment. The experiments were carried out with convectional Diesel and pure biodiesel from soy oil. The convectional Diesel used in this study is normally fuel found at gas stations and it has a cetane number of 43. The pure biodiesel used in this study was derived from a process of refining oil from soy oil and it has a cetane number of 38. The instrumentation within the shock tube used for the experiment included three pressure sensors (P1, P2 and P3), two temperature sensors (T3 and T1), a luminosity detection sensor (L1) and a fuel injector (FI). In the present work a mixture of the Nitrogen (N_2) and Argon (Ar) gases was used as the driver gas to obtain a longer test time. The **Figure 7** shows the position of the sensors, fuel injector, aluminum diaphragm location and mixture of the Nitrogen and Argon inlet in the shock tube.

The pressure sensor P3 (located at 1700 mm before the aluminum diaphragm) was used to monitor the pressure in the driver section and the diaphragm rupture pressure. The pressure sensor P2 (located at 700 mm after the aluminum diaphragm) was used to indicates the moment of passage of the shock wave after diaphragm rupture. This information is used to control and define the fuel injection timing. The pressure sensor P1 (located at 2700 mm after the diaphragm) was used to indicates the moment of passage of shock in region 1 where combustion occurs. For monitor the temperature in the driver section was used an analog temperature sensor T3. For monitor and control the temperature in the driven section was used a temperature sensor T1 with the same characteristics that the temperature sensor T3 used in driver section. The luminosity detection sensor L1 was used to indicates the

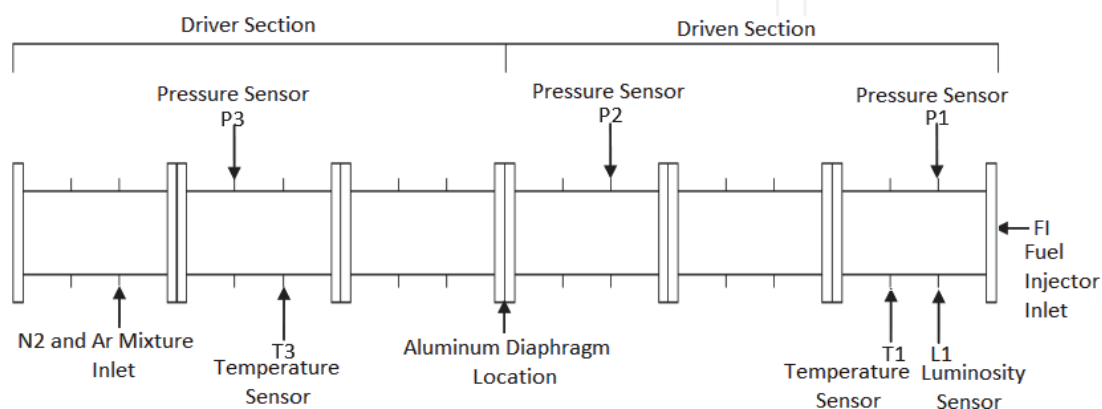


Figure 7. Position of the sensors, fuel injector, aluminum diaphragm location and mixture of the nitrogen and argon inlet in the shock tube (adapted from [17]).

moment of combustion. At the moment of ignition, the voltage of this sensor decreases in function of flame in shock tube. This information together with the pressure signal of P1 sensor was used to calculate the ignition delay time. The fuel injector FI injects fuel into the shock tube when the sensor pressure P2 detects the

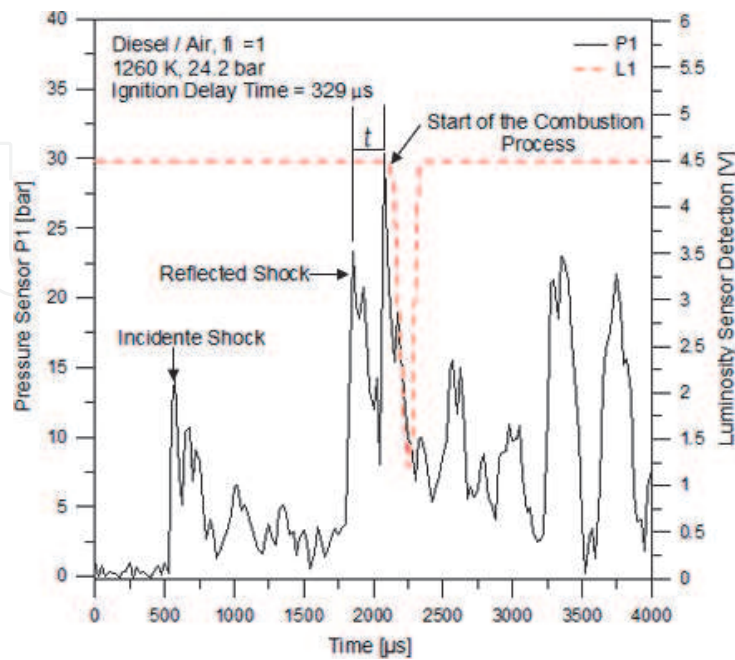


Figure 8. Ignition delay time of diesel in air at shock reflected pressure of 24.2 bar, equivalence ratio of 1 and temperature of 1260 K (adapted from [17]).

Incident shock		Reflected shock		Ignition delay time τ (μs)
P2 (bar)	T2 (K)	P5 (bar)	T5 (K)	
14.2	932	24.6	1150	362
14.2	945	24.3	1162	342
14	962	24.2	1260	329
13.7	874	23.6	940	603
14.2	912	23.8	1065	316
14.1	918	24.6	1082	418
13.9	915	23.1	980	443
13.4	902	24.2	1008	439
13.2	874	24.7	972	518
13.9	862	24.3	965	780
13.6	854	24.7	903	856
14	862	24.1	920	790
14.2	840	24.2	972	680
13.9	798	24.8	995	648
13.8	823	24.5	1040	490
13.6	890	23.8	1120	412
14	944	23.9	1243	325

Table 1. Measured ignition delay times for convectonal diesel in air (adapted from [17]).

passage of shock wave. The ignition delay time was calculated by the time difference between the passage of the shock wave by the P1 sensor and the start of the ignition detected by the luminosity detection sensor L1. The **Figure 8** shows a result of calculation of the ignition delay time of diesel measured in shock tube in air at shock reflected pressure of 24.2 bar, equivalence ratio of 1 and temperature of 1260 K.

The **Table 1** listed the measured ignition delay time τ for convectional diesel. All measurements were carried out equivalence ratios 1. The experiments were performed in the temperature range of 903 to 1260 K and target pressures were approximately 24 bar. Were found ignition delay times ranging from 316 to 856 microseconds.

Incident shock		Reflected shock		Ignition delay time
P2 (bar)	T2 (K)	P5 (bar)	T5 (K)	
14.6	942	24.7	1125	1356
14	918	24.4	960	1636
14.1	965	24.2	1150	945
13.2	932	23.6	995	1635
14.7	885	24.1	940	1525
14.3	948	24.5	1060	1567
13.9	935	23.2	1095	1470
13.4	842	24.7	916	1782
13.7	880	24.5	926	1678
14.7	982	24.8	1210	640
14.8	947	24.7	1180	982

Table 2.
 Measured ignition delay times for pure biodiesel from soybean oil in air (adapted from [17]).

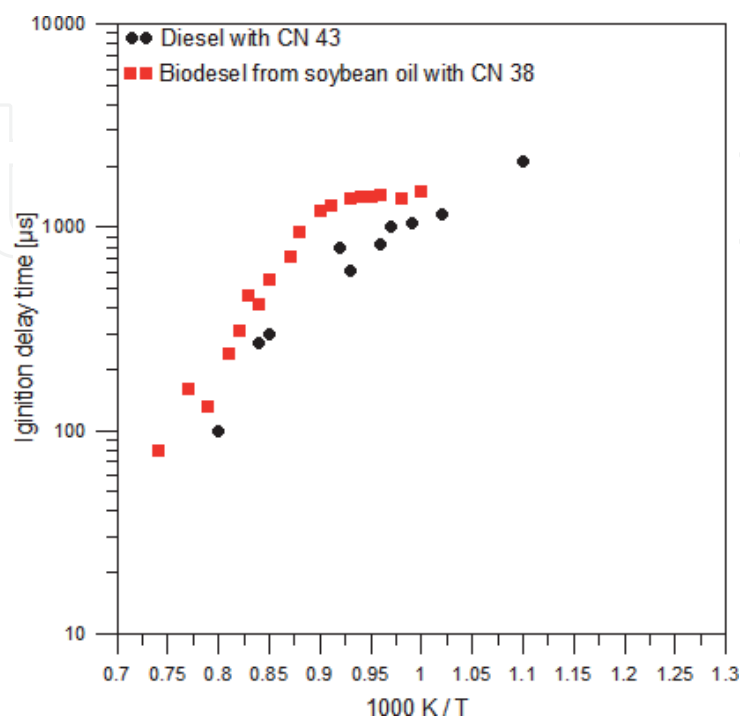


Figure 9.
 Ignition delay times for diesel and biodiesel from soybean oil in present study (adapted from [17]).

The **Table 2** listed the measured ignition delay time τ for pure biodiesel from soybean. All measurements were carried out equivalence ratios 1. The experiments were performed in the temperature range of 916 to 1210 K and target pressures were approximately 24 bar. Were found ignition delay times ranging from 640 to 1782 microseconds.

The **Figure 9** compare the ignition delay times for diesel and biodiesel from soybean oil measured in present study.

The ignition delay times measured in this study are consistent with those found in the literature. For convectional Diesel fuel were found times ranging from 316 to 856 microseconds and for biodiesel from soybean oil fuel were found times ranging from 640 to 1782 microseconds. These measured values are consistent with expectations since convectional Diesel has a higher cetane number than biodiesel from soybean oil. Convectional Diesel have a cetane number 43 while biodiesel from soybean oil have cetane number 38. This study confirm that the ignition delay time decreases with increasing cetane number. Fuel with a high cetane number has a short ignition delay time and the best quality in the combustion process.

Author details


Claudio Marcio Santana¹ and Jose Eduardo Mautone Barros^{2*}

¹ Federal University of Ouro Preto, Ouro Preto, Brazil

² University Federal of Minas Gerais, Belo Horizonte, Brazil

*Address all correspondence to: mautone@demec.ufmg.br

IntechOpen

© 2021 The Author(s). Licensee IntechOpen. This chapter is distributed under the terms of the Creative Commons Attribution License (<http://creativecommons.org/licenses/by/3.0>), which permits unrestricted use, distribution, and reproduction in any medium, provided the original work is properly cited. 

References

- [1] Sarathy, S. M., Farooq, A. and Kalghatgib, G. T., **Recent progress in gasoline surrogate fuels**, Progress in Energy and Combustion Science 65 (2018) 67–108, doi.org/10.1016/j.pecs.2017.09.004.
- [2] Glass, I. I., **Shock Tubes: Part I**. Toronto: University of Toronto, 1958.
- [3] Mcmillan, R.J. **Shock tube investigation of pressure and ion sensors used in pulse detonation engine research**, (2012), Corpus ID: 107883156.
- [4] H. J. Gordon, **Shock Tubes: Part II**. Toronto: University of Toronto, 1958.
- [5] L. R. Cancino, M. Fikri, A. A. M. Oliveira, C. Shulz, **Autoignition of gasoline surrogate mixtures at intermediate temperatures and high pressures: Experimental and numerical approaches**, Proceeding of the Combustion institute, 32 (2009) 501–508, doi:10.1016/j.proci.2008.06.180.
- [6] S. Niu, J. Zhang, Y. Zhang, C. Tang, X. Jiang, E. Hu, Z. Huang, **Experimental and modeling study of the auto-ignition of n-heptane and n-butanol mixtures**, Combustion and Flame 160 (2013) 31–39, doi:10.1016/j.combustflame.2012.09.006.
- [7] M. Fikri, J. Herzler, R. Starke, C. Schulz, P. Roth, G. T. Kalghatgi, **Autoignition of gasoline surrogates' mixtures at intermediate temperatures and high pressures**, Combustion and Flame 152 (2008) 276–281. doi:10.1016/j.combustflame.2007.07.010.
- [8] M. F. Campbell, S. Wang, C. S. Goldenstein, R. M. Spearrin, A. M. Tulgestke, L. T. Zaczek, D. F. Davidson, R. K. Hanson, **Constrained reaction volume shock tube study of n-heptane oxidation: Ignition delay times and time-histories of multiple species and temperature**, Proceedings of the Combustion Institute 35 (2015) 231–239. doi: 10.1016/j.proci.2014.05.001.
- [9] K. Y. Lam, Z. Hong, D. F. Davison, R. K. Hanson, **Shock tube ignition delay time measurements in propane / O₂ / argon mixtures at near-constant-volume conditions**, Proceeding of the Combustion Institute 33 (2011) 251–258.
- [10] S. M. Walton, D. M. Karwat, P. D. Teini, A. M. Gorny, M. S. Wooldridge, **Speciation studies of methyl butanoate ignition**, Fuel 90 (2011) 1796–1804.
- [11] B. Rotavera, E.L. Petersen, **Ignition behavior of pure and blended methyl octanoate, n-nonane and methylcyclohexane**, Proceeding of the Combustion Institute 34 (2013) 435–442.
- [12] C. K. Westbrook, C. V. Naikb, O. Herbinetc, W. J. Pitz, M. Mehla, S. M. Sarathya, H. J. Currand, **Detailed chemical kinetic reaction mechanisms for soy and rapeseed biodiesel fuels**, Combustion and Flame 158 (2011) 742–755, doi: 10.1016/j.combustflame.2010.10.020.
- [13] D.F. Davidson, Y. Zhu, J. Shao, R.K. Hanson, **Ignition delay time correlations for distillate fuels**, Fuel 187 (2017) 26–32. doi.org/10.1016/j.fuel.2016.09.047.
- [14] V. N. Hoang, L. D. Thi, **Experimental study of the ignition delay of diesel and biodiesel blends using a shock tube**, Biosystems engineering 134 (2015) 1–7. doi.org/ 10.1016/j.biosystemseng.2015.03.009.
- [15] S. Gowdagiri, M. A. Oehlschlaeger, **Global Reduced Model for Conventional and Alternative Jet and**

Diesel Fuel Autoignition, Energy Fuels
28 (2014) 2795–2801. doi.org/10.1021/
ef500346m.

[16] G. Flora, J. Balagurunathan, S.
Saxena, J. P. Cain, M. S. P.
Kahandawala, M. J. DeWitt, S. S.
Sidhua, E. Corporan, **Chemical ignition
delay of candidate drop-in
replacement jet fuels under fuel-lean
conditions: A shock tube study**, Fuel
209 (2017) 457–472. doi.org/10.1016/
j.fuel.2017.07.082.

[17] Santana, C.S., Barros, J. E. M.,
Junior, H. A. A, Braga, J. O. and Neto, J.
C. B, **Measuring and comparing the
ignition delay time of the reference
diesel, convectional diesel, additive
ethanol and biodiesel from soybean
oil using a shock tube**, Journal of the
Brazilian Society of Mechanical Sciences
and Engineering (2020) 42:102, doi:
10.1007/s40430-020-2183-z.